

An Approach for the Accurate Investigation of Full-Scale Ship Boundary Layers and Wakes

Blanca Pena, Ema Muk-Pavic, Giles Thomas, Patrick Fitzsimmons

Department of Mechanical Engineering, University College London, London WC1E 7JE, UK

Abstract: Existing recommended practices in the literature do not provide clear and concise guidance for the selection of the most suitable numerical modelling strategy for investigating the boundary layer around a ship at full scale. For example, the International Towing Tank Conference procedure for calculating the nominal wake fields of full-scale ships does not clearly specify which turbulence modelling approach should be used to accurately represent the near-wall flow in the ship's aft region.

This paper presents a numerical approach that can accurately represent the boundary layer of full-scale ships. Three turbulence modelling strategies, suitable for the simulation of ship flows, have been assessed: $k-\epsilon$, $k-\omega$ SST RANS and an IDDES formulation. Results from each method have been compared against the full-scale ship propeller torque data of the MV Regal, a 138m long general cargo vessel. Additionally, the capability of each turbulence strategy to resolve time-dependent features of the flow, such as the bilge vortex and its effect on the boundary layer velocity fields, has been evaluated.

The results from this investigation show that the IDDES based numerical model replicated the sea trials measurements with the highest degree of accuracy. Furthermore, this study confirmed that the choice of turbulence strategy has a major impact on the full-scale velocity fields in the aft region of a ship.

Keywords: hydrodynamics; full scale; ship turbulence modelling; vorticity; CFD.

1 Introduction

Due to the recent IMO CO₂ reduction legislation (IMO, 2020) there is a need to be able to accurately evaluate the hydrodynamic performance of Energy Saving Devices (ESDs) during the design process. Currently, this can be problematic since there is no consensus on the most appropriate numerical approach to accurately predict the performance of ESDs before the actual full-scale sea trials. Existing numerical methods exhibit shortcomings that need to be overcome, such as scaling and accurately modelling the turbulence contained in the boundary layer and wake, prior to being used with confidence. This is especially important since the majority of ESDs are situated at the aft region of a ship where the boundary layer and wake are most pronounced. The most established guidance for calculating nominal wakes using Computational Fluid Dynamics (CFD) is provided by the International Towing Tank Conference (ITTC) in ITTC 7.5-03-03-02 (ITTC, 2014c) which establishes that: *'At full-scale the bilge vortex on full form ship becomes less pronounced, and there is practically no bilge vortex distortion (hook shape) present at propeller disc, the difference in the predicted wake pattern between the advanced turbulence models and linear eddy viscosity models tends to decrease, so there is a wider freedom in choosing turbulence models'*. The ITTC also notes that existing turbulence models have not yet been sufficiently validated against full-scale data to provide confidence in their use.

Research to investigate full-scale ship boundary layer simulation procedures using Navier-Stokes CFD methods was carried out at the 2000 Gothenburg Workshop in Ship Hydrodynamics (Larsson et al., 2003). This workshop compared the impact of Reynolds Averaged Navier Stokes (RANS) and Detached Eddy Simulation (DES) turbulence modelling approaches in calculating nominal wakes for different geometries at full scale and model scale. In general, the workshop participants agreed that at full scale the propeller region flow is minimally influenced by the turbulence modelling approach, which is in line with the ITTC 7.5-03-03-02 procedure (ITTC, 2014c).

The EFFORT study (Starke et al., 2006) evaluated the accuracy of various RANS prediction methods including the Reynolds Stress Model (RSM) approach) for simulating the flow around different full-

scale ship geometries. This study concluded that boundary layer flow predictions in full scale require advanced turbulence models that account for the anisotropy of the flow, thus contradicting the findings from the 2000 Gothenburg Workshop. The lack of consensus between Starke et al. and the 2000 Gothenburg Workshop may be due to the rapid improvement in computational capacity between the investigations, for example Starke et al. discretised the computational domain using significantly finer meshes than would have been feasible at the time of the Gothenburg workshop in 2000.

Full-scale flow predictions using the original Detached Eddy Simulation (also known as DES97) and its improved version, the Delayed Detached Eddy Simulation (DDES), were conducted by Xing et al. (2010) during the 2010 Gothenburg Workshop on CFD in Ship Hydrodynamics (Larsson et al., 2013). The authors established that both the DES97 and the DDES improve the prediction of the total resistance and velocity distribution across most of the propeller plane, except in the region close to the symmetry plane. The authors also found that both the DDES and DES models had issues in accurately predicting the shear stress in the boundary layer region. These issues might be attributable to the log-layer mismatch behaviour that DES97 and DDES models typically exhibit (Spalart *et al.*, 2006) and which could be corrected using an Improved Delayed Detached Eddy Simulation (IDDES) approach; which represents an improved version of the DDES and DES97 approaches (Shur *et al.*, 2008).

More recently, Lloyds Register organised a workshop on full-scale ship hydrodynamics to assess the accuracy of the latest CFD simulations of ship hydrodynamics (Lloyds Register, 2016). This workshop provided an opportunity for over 20 organisations to conduct blind comparisons of their full-scale resistance and self-propulsion numerical models with full-scale sea trials measurements. Whilst this workshop did not focus on boundary layer investigations, the availability of the full-scale measurements data allowed the many CFD approaches to be validated at full scale.

This paper reports on an investigation into determining which numerical approach can most accurately represent a ship's boundary layer at full-scale. Two turbulence modelling approaches, suitable for the simulation of ship flows have been assessed: the $k-\epsilon$ and $k-\omega$ Shear Stress Transport or

SST RANS. These commonly used modelling approaches were compared for the first time against the IDDES approach, the improved version of the DDES that Xing et al. studied at full-scale during the 2010 Gothenburg Workshop (Larsson et al., 2013). Of particular relevance is that this work uses very fine meshes and sophisticated turbulence modelling strategies that were not computationally feasible or available at full-scale at the time of the Starke et al. (2006), Xing et al. (2010) and 2000 Gothenburg Workshop investigations (Larsson et al., 2003). For the first time, this study critically assesses the suitability of each turbulence strategy to study the hydrodynamic performance of propellers, rudders and energy saving devices that work within the boundary layer limits and wake of a ship. Additionally, this study looks into the capability of each numerical approach to resolve detailed time-dependent features of the flow, such as the bilge vortex development and its effect on the boundary layer velocity fields. The work is based on the same data used at the Lloyds Register Workshop (2016) (ship geometry and sea trial measurements) to enable the validation of the numerical model.

This paper is organised as follows: in section 2, a description is given of the case study ship and the experimental benchmark data used for validation purposes; section 3 covers the numerical strategy used for the computations of the unsteady flow calculations; section 4 details the set-up and computational mesh; the final sections provide the results and discussion, as well as conclusions and suggestions for future work.

2 Benchmark Case Study

The physical case used for this investigation was the general cargo carrier *Regal* (Lloyds Register, 2016). This is a 138m single screw vessel (Figure 1 and Figure 2) with the following main particulars (Table 1):

Table 1 *Regal* Main Particulars (Lloyds Register, 2016)

Parameter	
Length between perpendiculars, L_{pp}	138 m
Breadth moulded, B	23 m
Depth moulded, D	12.1 m
Draught, T	Ballast
Propeller diameter, D	5.2 m (four-bladed)
Longitudinal Centre of Gravity, LCG	71.2 m (from A.P)
Vertical Centre of Gravity, VCG	0 m (free surface)
Transverse Centre of Gravity, TCG	0 m
Displacement, Δ	12881 tonnes
Pitch Radius of Gyration, R_{yy}	0.25 L_{pp} m

Before the sea trials, the vessel was dry-docked, the hull was cleaned, and the propeller surface was polished. In this clean condition, the hull, rudder, and propeller were scanned with 3D lasers to obtain accurate geometric representations. The scanned geometries were directly imported into the CFD computations, ensuring high accuracy of the geometry CAD models (rather than relying on the design drawings).



Figure 1 *Regal* general cargo ship (Lloyds Register, 2016)

The sea trials were conducted in a reasonably calm condition, as recommended by the ISO 15016:2015 (2015), with the *Regal* at the ballast draught for three different shaft speeds of 71.6, 91.1

and 106.4 rpm following the ITTC 7.5-04-01-01.1 procedure for sea trials (ITTC, 2014b). During each test run the power, ship speed and shaft torque were recorded. More details of the sea trials can be found in the workshop’s proceedings (Lloyds Register, 2016).

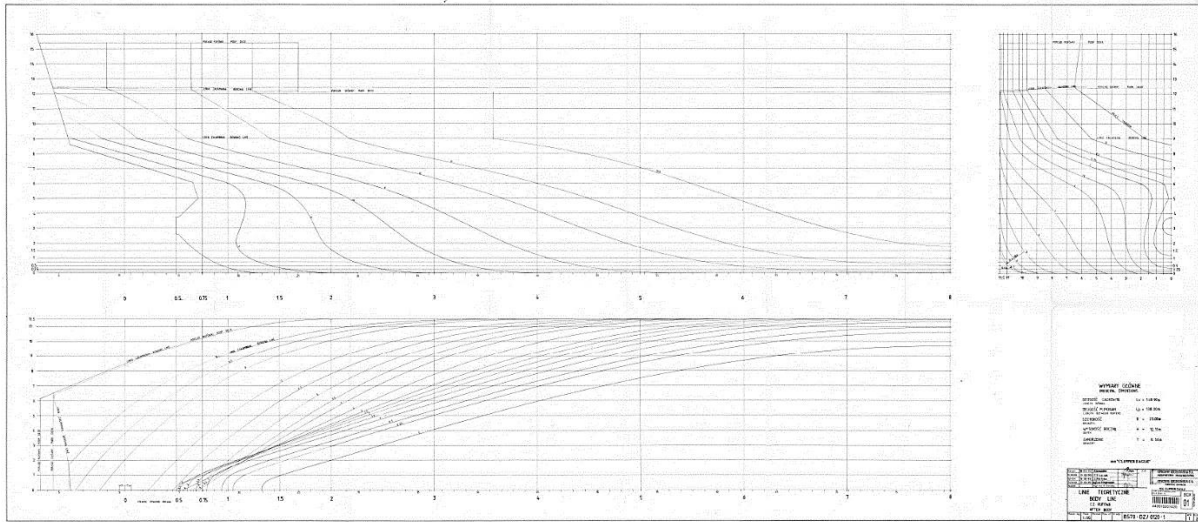


Figure 2 *Regal* hull lines plan (Lloyds Register, 2016)

3 Numerical Approach

The scope of the analysis corresponds to the programme conducted during the Lloyds Register full-scale Hydrodynamics workshop (Lloyds Register, 2016). The numerical simulations of the flow around the ship were conducted using the commercial CFD code Siemens Star CCM+ on an HPC parallel multi-node Linux cluster, using up to 200 cores simultaneously. The following numerical experiments were undertaken for the full-scale ship *Regal* at the ballast draft and in a clean hull condition:

- a) Bare hull simulations (with the rudder as the only appendage) at the range of speeds given in Table 2. This set of simulations significantly reduced the complexity of the aft end flow (compared with self-propulsion tests) and allowed the nominal wake fields to be studied.

Table 2 Bare-Hull Simulation Conditions

Speed (knots)	Re	Fr
8	6.43E+08	0.11
10	8.03E+08	0.14
12	9.64E+08	0.17
14	1.12E+09	0.20

b) Self-propulsion simulations (with the propeller and rudder) at three different shaft speeds: 71.6, 91.1 and 106.4 rpm, corresponding to the ship speed measured during the sea trials (as shown in Table 3). This set of self-propulsion test simulations were used to validate the accuracy of the set-up by comparing the numerically obtained torque with that measured during the sea trials. It is assumed that a satisfactory agreement of the simulated torque with the sea trials measurements will give strong confidence that the hydrodynamics of the boundary layer has been accurately resolved.

Table 3 Self-Propulsion Simulation Conditions Matching with the Lloyds Register Sea Trials Speed
(Lloyds Register, 2016)

Shaft Speed (rpm)	Speed (knots)	Re	Fr
71.6	9.25	7.43E+08	0.13
91.1	11.60	9.32E+08	0.16
106.4	13.00	1.04E+09	0.18

3.1. Turbulence Modelling Strategies

In this study, three turbulence modelling strategies were investigated (Table 4):

Table 4 Turbulence Modelling Strategies

Set-up	Turbulence Strategy	Strategy Group	Notes
Set-up 1	Realisable k- ϵ	RANS	Curvature correction implemented once convergence is achieved.
Set-up 2	SST Menter k- ω	RANS	Curvature correction implemented once convergence is achieved.
Set-up 3	IDDES	DES	Coupled with k- ω SST and curvature correction

Set-up 1- RANS k- ϵ is based on the k- ϵ turbulence model that is widely used in ship hydrodynamic analysis, as it gives satisfactory results for many generic ship flow problems. However this model is recognised to lack sensitivity to adverse pressure gradients and tends to over-predict the shear-stress levels near the wall. Due to the limitations of this model it is possible that flow separation may not be appropriately modelled (Menter, 1993).

Set-up 2 – RANS Shear Stress Turbulence or SST is based on the k- ω formulation as proposed by Menter (Menter, 1993), which combines the k- ω turbulence model in the near-wall region with the k- ϵ turbulence model in the free shear flow. This model is a well-respected turbulence approach commonly used for ship hydrodynamics simulations, in particular for modelling flow prone to separation.

Set-up 3- The IDDES is based on the model developed by Shur et al. (Shur *et al.*, 2008) which switches between the RANS SST k- ω model, in the region near the no-slip wall, and Large Eddy Simulation (LES) in the wake region to model the larger scale eddies such as the bilge vortex. This model requires a fine mesh of higher quality than the turbulence modelling strategies described above (set-ups 1 and 2) and has proven to be accurate during self-propulsion tests (Pena et al., 2019)

The IDDES approach is obtained by modifying the dissipation term of the transport equation for the turbulent kinetic energy (k). After introducing a length scale, L_{hybrid} , the turbulence model equations in the tensor form are given as (Shur *et al.*, 2008):

$$\frac{\partial(\rho k)}{\partial t} + \frac{\partial(u_j k)}{\partial x_j} = \frac{\partial}{\partial x_j} \left[(\mu_l + \sigma_k \mu_t) \frac{\partial k}{\partial x_j} \right] + \tau_{ij} S_{ij} - \frac{\rho k^{3/2}}{L_{hybrid}} \quad (1)$$

$$\frac{\partial(\rho \omega)}{\partial t} + \frac{\partial(\rho u_j \omega)}{\partial x_j} = \frac{\partial}{\partial x_j} \left[(\mu_l + \sigma_\omega \mu_t) \frac{\partial \omega}{\partial x_j} \right] + \alpha \frac{\omega}{k} \tau_{ij} S_{ij} - \frac{\rho k^{3/2}}{L_{hybrid}} - \beta \rho \omega^2 + 2(1 - F_1) \frac{\rho \sigma_{\omega 2}}{\omega} \frac{\partial k}{\partial x_j} \frac{\partial \omega}{\partial x_j} \quad (2)$$

where S_{ij} represents the strain tensor, τ_{ij} the stress tensor, ρ is the fluid density, ω represents the specific dissipation rate, μ_t the turbulent eddy viscosity, μ_l the dynamic viscosity, $\sigma_{\omega 2}$ is a model coefficient and F_1 is the blending function. The length scale, L_{hybrid} is defined as

$$L_{hybrid} = f_B(1 + f_e)L_{RANS} + (1 - f_B)L_{LES} \quad (3)$$

where $L_{RANS} = k^2/(\beta^* \omega)$, β^* is given in k- ω Model Coefficients taken as 0.09. $L_{LES} = C_{DES} \Delta$, where $C_{DES} = 0.78$, and Δ is the grid length scale. The elevating-function f_e prevents an excessive reduction of the RANS Reynolds Stresses (Shur *et al.*, 2008). The main feature of this model is the empirical blending-function, f_B , which presents a switching function from RANS ($f_B = 1$) to LES model ($f_B = 0$).

It is also known that the RANS SST Menter and k- ϵ turbulence approaches are insensitive to stabilising and destabilising effects usually associated with large (streamline) curvature and frame-rotation (Menter, 1993). These effects can be accounted for by using a curvature correction factor, which is a function of the strain rate tensor and the rotation-rate tensor and alters the turbulent kinetic energy production terms according to the local rotation and vorticity rates (Arolla and Durbin, 2013). This curvature correction has been shown to significantly improve the calculation of the ship hydrodynamic flow physics (Andersson *et al.*, 2015).

3.2. Numerical Model of the Ship

The ship model was placed in a prismatic fluid domain with the inlet boundary placed one length upstream of the bow, the outlet boundary two ship lengths downstream of the ship's stern and the sides of the fluid domain one ship length towards the port and the starboard sides, as shown in Figure 3 (left). This approach follows the ITTC recommended practices (ITTC, 2014c, Lloyds Register, 2016). A Dirichlet condition was imposed on the inlet. The DFBI (Dynamic Fluid Body Interaction) module was used to simulate the motion of the ship in response to pressure and shear forces exerted by the fluid on the solid body, as well as gravity. The ship was allowed to sink and trim freely, by calculating the resultant force and moment acting on the ship, and solving the governing equations of rigid body motion every time-step to find the new position of the rigid body. The physical properties of *Regal*, such as the centre of gravity, inertia and displacement that are defined in the simulation correspond to the values determined during the sea trials as shown in Table 1.

In order to simulate the propeller action, the calculation is performed with an imposed flow speed, corresponding to the mean speed (measured during the trials), and the propeller rpm modelled by the MRF (Multiple Reference Frame) approach. Once the free surface has converged, the propeller RBM (Rigid Body Motion) or '*sliding mesh*' is activated, so the propeller starts rotating. This approach has provided accurate results during numerical-self propulsion tests (Ponkratov and Zegos, 2015). Lastly, the imbalance of longitudinal forces between propeller thrust and effective ship resistance are noted, and the free-stream speed is adjusted (if needed) to minimise the imbalance of these forces.

3.3. Modelling the Ship's Superstructure

A sensitivity analysis was conducted with and without the superstructure to confirm that the impact of the superstructure on the simulation results could be disregarded. In both cases, the superstructure presence was taken into account in the ship parameters: displacement, trim and radii of gyration. The study showed that including the superstructure geometry did not have a substantial impact on the resultant torque, sinkage and trim. The superstructure resistance was estimated to be around 3% of the

total ship resistance; this outcome is in agreement with the 2016 Hydrodynamic Workshop (Lloyds Register, 2016) as the superstructure resistance was estimated by most participants of the workshop to be between 2 and 4% of the total resistance. The majority of studies found in the literature neglect the superstructure without reporting a significant difference in their torque or thrust self-propulsion results (Ponkratov and Zegos, 2015 , Jasak *et al.*, 2019). Therefore, the superstructure geometry was not included in the CFD computations.

4. Computational Set-up

4.1 Time-step and Convergence Criteria

The Courant number (C_r) is used to represent the number of cells that the fluid travels through within a time-step, and is defined as $C_r = \frac{u\Delta t}{\Delta x}$ (where u is the local speed, Δt the interval of time (time-step) and Δx the cell size in the direction of the flow). A mean C_r of 1, which gives a propeller rotation of approximately 1 degree per time-step, was implemented ensuring the accuracy and stability of the simulations. All simulations used a 2nd order temporal and spatial discretisation for all equations.

The simulation convergence was monitored for residuals and hydrodynamic torque coefficient (K_Q) and thrust coefficient (K_T). These coefficients are defined as $K_Q = \frac{Q}{\rho n^2 D^5}$ and $K_T = \frac{T}{\rho n^2 D^4}$ where Q is propeller torque, T is the propeller thrust, ρ is the fluid density, n is shaft revolutions and D propeller diameter.

4.2 Mesh

A hexahedral un-structured mesh type was used to discretise the fluid domain with local refinements at the regions of particular interest and where a more detailed resolution of the flow was required. The refinement was made within the wedge region around the ship (Figure 5 left) and the bow (Figure 4

right) to capture flow around the hull and wave pattern (Figure 5 left); with further refinements around the stern of the vessel (Figure 3 right) as well as the rudder (Figure 4 right). For the self-propulsion simulation only, a separate cylindrical sub-domain was created for the propeller to allow the rigid body rotation to be modelled (Figure 4). Internal interface boundary conditions were implemented on the cylinder boundary surfaces between the rotating and static domains.

With regard to the free surface, the volume of fluid method was used to capture the deformation of the free surface. In addition, a second-order spatial resolution scheme was used to discretise the free surface, with a trimmed mesh aligned with the calm water free surface. The near-wall cell was meshed achieving a y_+ of 1 and ensuring that no-wall functions are applied in the domain.

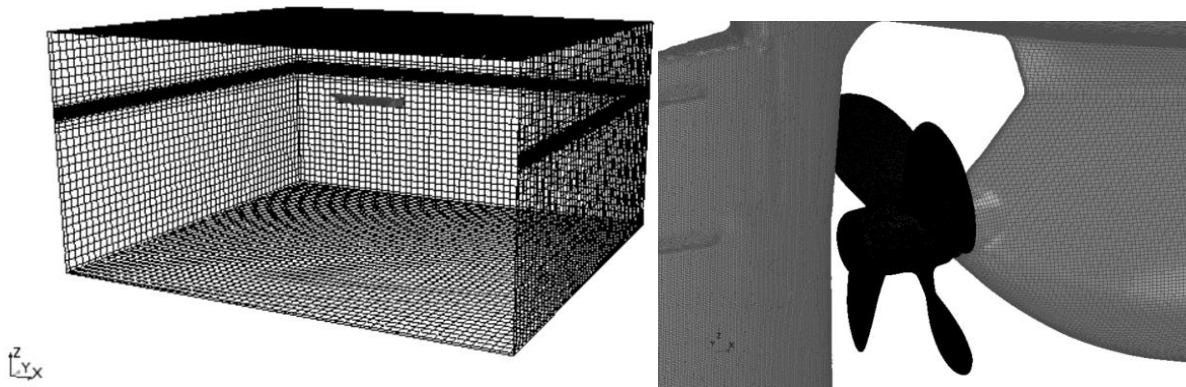


Figure 3 Fluid domain (left). Stern mesh showing the propeller refinements (right)

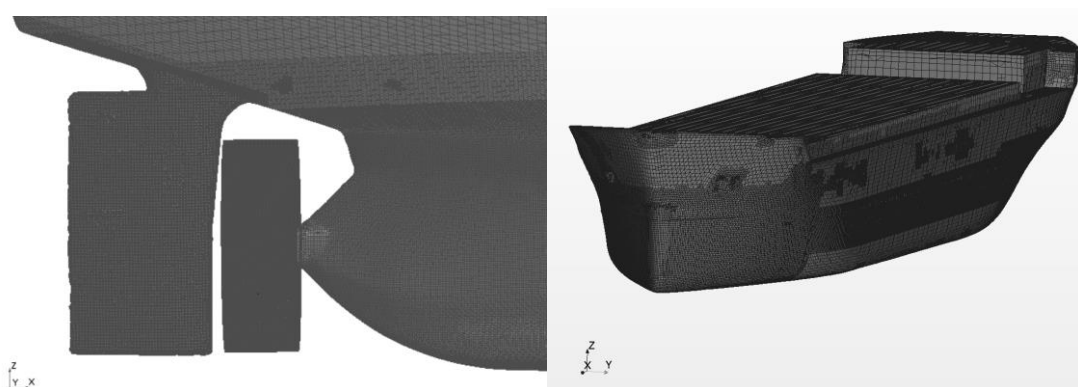


Figure 4 Propeller rotating cylinder (left) and bow refinements (right)

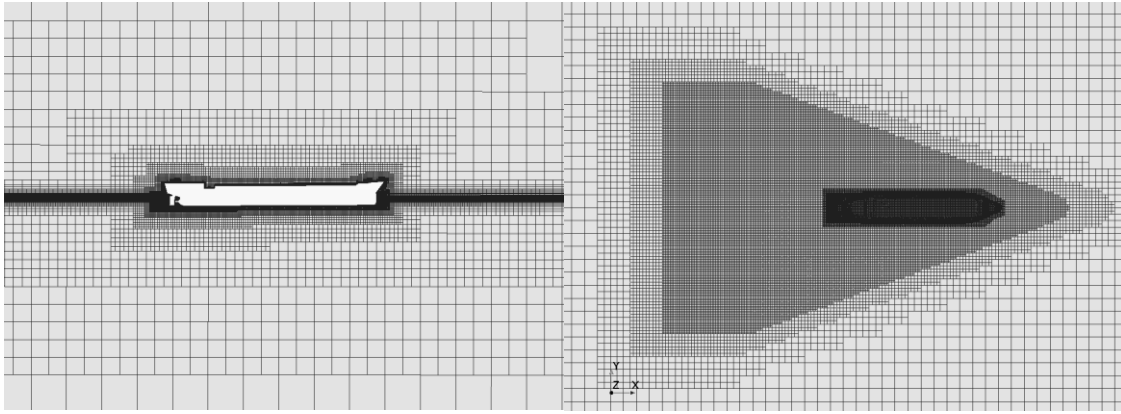


Figure 5 Mesh in the region of free surface and wake: centreline side view (left), plan view (right)

5. Mesh Independence Study

A mesh independence study was conducted for the IDDES self-propulsion set-up, as this was the most demanding case of the three self-propulsion simulations, while monitoring the convergence of K_Q and K_T following recommended practices (ITTC, 2017). The assumption was that if the results proved to be mesh independent for the most demanding set-up (the IDDES), it would also be mesh independent for the RANS numerical set-ups. This assumption was confirmed by conducting a mesh sensitivity study for the RANS cases (Section 5.1).

The mesh independence study was conducted on four different grid resolutions by varying the mesh size input parameter while holding all other parameters constant. The uniform parameter refinement ratio was established as $\sqrt{2}$. Table 5 shows the results for the torque coefficient and the convergence ratio. The convergence ratio between meshes 3 and 4 was only 1.45% and 1.13% for K_Q and K_T respectively, and therefore the mesh independence was confirmed.

Table 5 Mesh Independence Study for the Self-Propulsion Simulation Case: Set-Up 1 (IDDES) at 71rpm

Mesh Name	Million Elements	K_Q	K_Q Convergence Ratio	K_T	K_T Convergence Ratio
1.Coarse	25	2.01E-03	-	1.84E-02	-
2.Medium	35	1.88E-03	-6.60%	1.75E-02	-4.74%
3.Fine	50	1.83E-03	-2.63%	1.72E-02	-2.21%
4.Finest	71	1.80E-03	-1.45%	1.70E-02	-1.13%

5.1. Mesh Sensitivity Study for the RANS Set-ups

A sensitivity study was conducted to check that the IDDES set-up was mesh independent when changing to RANS turbulence models. The 50M mesh was subjected to a global element refinement, creating a 71M element mesh. As shown in Table 6 and Table 7, the solution for the torque and thrust coefficient varies within 1%. Therefore, the set-up was deemed mesh independent for the RANS set-ups.

Table 6 Set-Up 2 (SST) Self-Propulsion Set-Up Mesh Sensitivity Study at 71 rpm

Mesh Name	Million Elements	K_Q	K_Q Convergence Ratio	K_T	K_T Convergence Ratio
1.SST	50	1.76E-03	-	1.73E-02	-
4.SST Finer	71	1.75E-03	0.43%	1.72E-02	-0.56%

Table 7 Set-up 3 (k- ϵ) Self-Propulsion Set-Up Grid Sensitivity Study at 71 rpm

Mesh Name	Million Elements	K_Q	Convergence Ratio	K_T	K_T Convergence Ratio
1. k- ϵ	50	1.69E-03	-	1.74E-02	-
4. k- ϵ Finer	71	1.66E-03	-1.04%	1.76E-02	1.11%

6. Uncertainty Analysis

A mesh uncertainty analysis was successfully conducted following the ITTC Quality System Manual Recommended Procedures and Guidelines 7.5-03-01-01 (ITTC, 2017). Table 8 shows the analysis results where: R_G is convergence ratio, p_G order of accuracy, C_G correction factor, U_G grid uncertainty, δ^*_G estimated error, U_{GC} corrected grid uncertainty, S_C corrected simulation value, U_{SN} numerical uncertainty, U_V validation uncertainty. U_G , δ^*_G and U_{GC} are given as a % of the mesh independent torque coefficient value. U_{SN} and U_V are provided as a percentage of the measured experimental data (%D). From the results, it can be seen that monotonic convergence was achieved ($0 < R_G < 1$), with an order of accuracy P_G of 1.79, which was less than the recommended order of accuracy of 2 and therefore resulting in high confidence (ITTC, 2017). These results indicated that the solution was in the asymptotic range and no further refinements were needed.

The final verification of the set-up was conducted by performing a comparison between the simulation predictions and the sea trial data. In this case, the error was estimated as 2% with a validation uncertainty of 2.22%. In this case the validation uncertainty was higher than the error between the simulations and the experimental data ($E < U_V$). Therefore, the set-up was considered validated for further analysis.

Table 8 Set-up 1 (IDDES) Self-Propulsion Set-Up Mesh Uncertainty Analysis of the Torque at 71rpm

Simulation Name	R_G	P_G	C_G	U_G [%D]	δ^*_G [%D]	U_{Gc} [%D]	S_C	U_{SN} [%D]	U_{Vc} [%D]	E [%D]
IDDES	0.55	1.79	0.86	1.75	1.50	0.20	1.77E-03	1.68	2.22	2.10

7. Results and Discussion

The numerical results are shown and discussed in the following three subsections. Firstly, K_Q , from the self-propulsion set-up is directly compared to the sea trials propeller torque measurements. The next subsections compare and discuss the results of the bare-hull numerical set-up for vorticity and

nominal wake fields, at the stern of the ship, for the three different numerical approaches. The results are referenced to a right-hand cartesian coordinate system with the origin at the intersection of the aft perpendicular and the waterplane with positive axis directions from bow towards the stern, centre-plane towards the port side and from the free surface upwards.

7.1 Torque Coefficient

Figure 5 compares the torque coefficients obtained at the self-propulsion point, using the three different turbulence modelling strategies, against the experimental values measured on the sea trials. All three numerical models were able to produce consistent results compared with the experimental data; with 8% difference for the $k-\epsilon$ and 5% difference for the SST. The IDDES was the most accurate of the three set-ups, being able to produce a maximum deviance of 2% from the sea trials measurements. The higher accuracy of the IDDES numerical model was expected, and it is due to the IDDES model mesh being strategically defined to allow for the large unsteady bilge vortex to be resolved from the Navier-Stokes equations. In general, the isotropy assumption near the wall is not expected to significantly impact on the results since at high Reynolds numbers the small scale turbulent motions tend to be statistically isotropic (Kolmogorov, 1941). By contrast, the $k-\epsilon$ and the SST set-ups modelled all turbulent scales contained in the flow (including the bilge vortex) by using the averaged Navier-Stokes equations, as well as by considering the isotropy assumption of the viscous stress tensor. These assumptions are expected to be the main reason for the higher deviances of the RANS set-ups when compared to the sea trials data. Therefore, the numerical model's torque coefficient comparison has proven that the hydrodynamics of the ship boundary layer and wake were accurately modelled for the IDDES case. This conclusion is reasonable due to the good agreement achieved by the IDDES torque coefficient and the sea trials measurements.

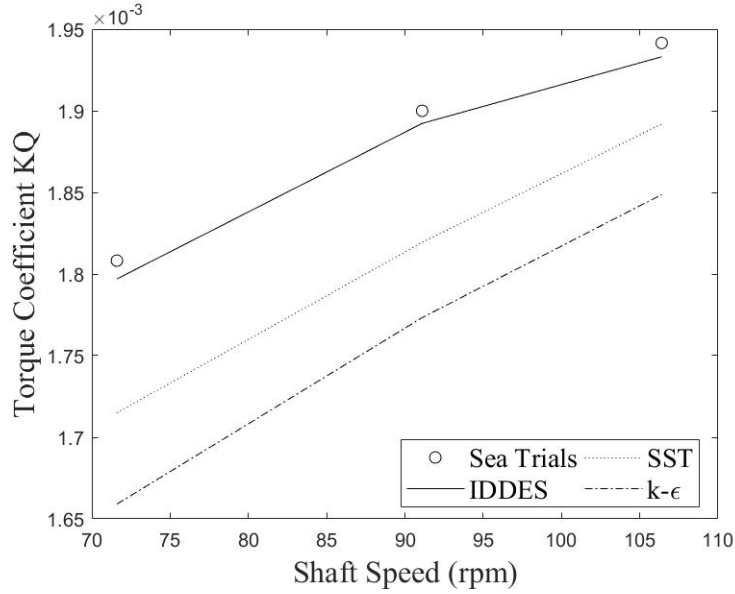


Figure 6 K_Q for the three turbulence modelling strategies and the experimental measurements at three shaft speeds

7.2 Vorticity and Vortex Shedding

Figure 7 shows snapshots of the instantaneous vortex core locations shed from the hull. These vortex structures are represented using positive isosurfaces of the Q Criterion $Q = \frac{1}{2}(\Omega_{ij}\Omega_{ij} - S_{ij}S_{ij})^{1/2}$, where Ω is the rotation tensor and S represents the strain tensor (Jeong and Hussain, 1995). The isosurfaces are coloured by non-dimensional axial velocity. The main vortex structures shed from the hull are the side vortex and the bilge vortex.

With regard to the side vortex (Figure 7), it is seen that all three set-ups were able to predict it. However, the location and dimensions are dependent upon the chosen turbulence modelling strategy. Although no PIV measurements of the side vortex on full-scale ships are available, this finding is consistent with experiments and computations over bluff bodies such as cylinders (Nishino et al., 2008). For the bilge vortex (Figure 7), a clear difference between the three cases can be seen: the IDDES model was able to predict vortex shedding ring-like structures behind the hull, whereas the k-ε and the SST Menter represent the longitudinal vortex as a straight vortex tube. The IDDES ring-like

structures were expected, and they appear as a consequence of instabilities of the shear layer arising at the boundary between the slow wake flow passing by the hull and the free-stream flow (Doligalski, 2002). This phenomenon has been further confirmed by experiments with blunt bodies (Sakamoto and Haniu, 1990; Dousset and Poth erat, 2010) and it has been reported in towing tank model scale tests (Thornber *et al.*, 2010). The reason why the two-equation turbulence models are not able to calculate the ring-like structures is well known. While the application of a standard RANS model in unsteady mode results in a single frequency vortex shedding, the implementation of the IDDES allowed mimicking of the break-up of the large turbulent scale vortices into smaller turbulent scales vortices, also known as the '*energy cascade*' (Pope, 2000). This implies that the IDDES approach could be advantageous when predicting the correct mixing behind a ship and when extracting spectral information needed during ship-induced vibrations or noise assessments.

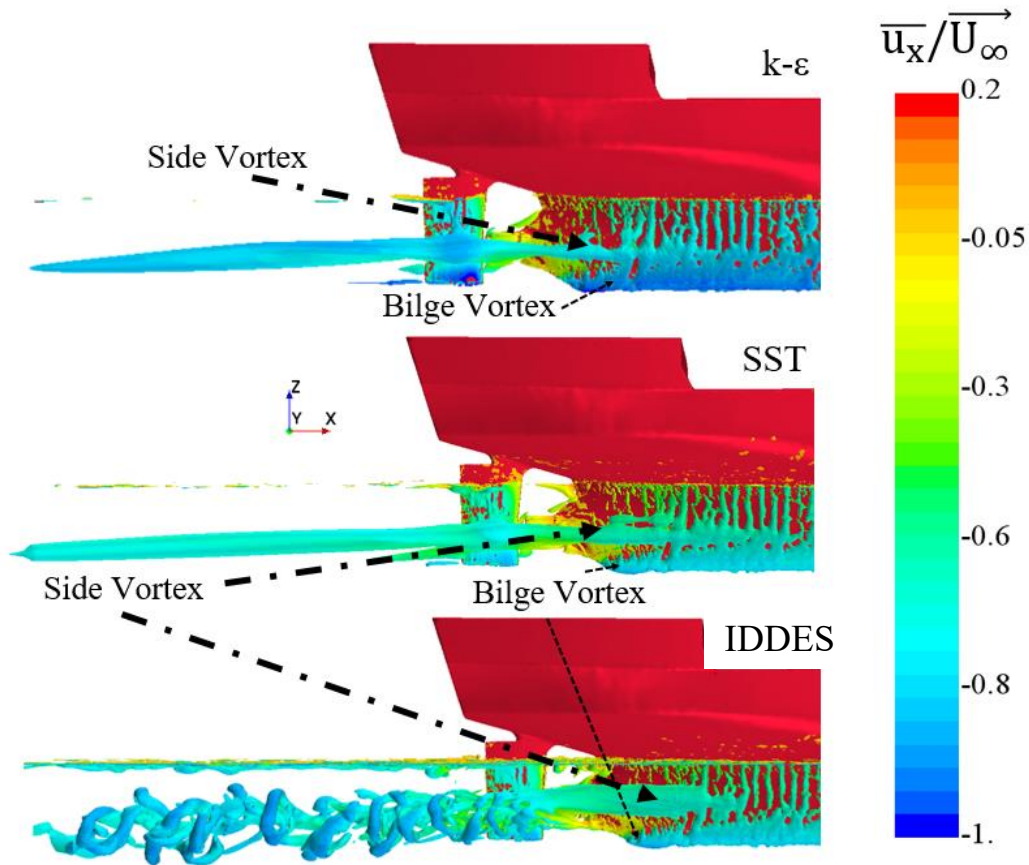


Figure 7 Iso-surfaces of positive Q-criterion coloured by streamwise non-dimensional speed for the three turbulence modelling strategies.

Contours of instantaneous streamwise vorticity from the RANS and IDDES set-ups are shown in Figure 8. The vorticity plots were taken at a distance of $x/L = 0.03$ from the aft perpendicular, being the region directly upstream of the propeller. The comparison shows that the three set-ups were able to calculate the bilge vortex; however, the IDDES approach modelled a significantly higher vortex strength. Additionally, the IDDES vorticity fields show Kelvin-Helmholtz instabilities shed from the keel. This phenomenon is consistent with model scale ship towing tank experiments (Aloisio G., 2006). Also, higher definition of secondary and tertiary vorticity in the near-wall region was observed for the IDDES set-up. These secondary and tertiary vortex structures were induced by a strong primary vortex, being expected due to the IDDES capability of resolving larger-scale eddies. These results once again suggest that the IDDES can provide a higher definition of the vorticity that RANS

was not able to determine. Such a detailed definition of the vorticity fields is particularly important when designing structures or devices that are placed within the boundary layer of the ship and wake. In particular, the assessment of the performance of energy saving devices or propellers depends on the flow structure within the region where they work.

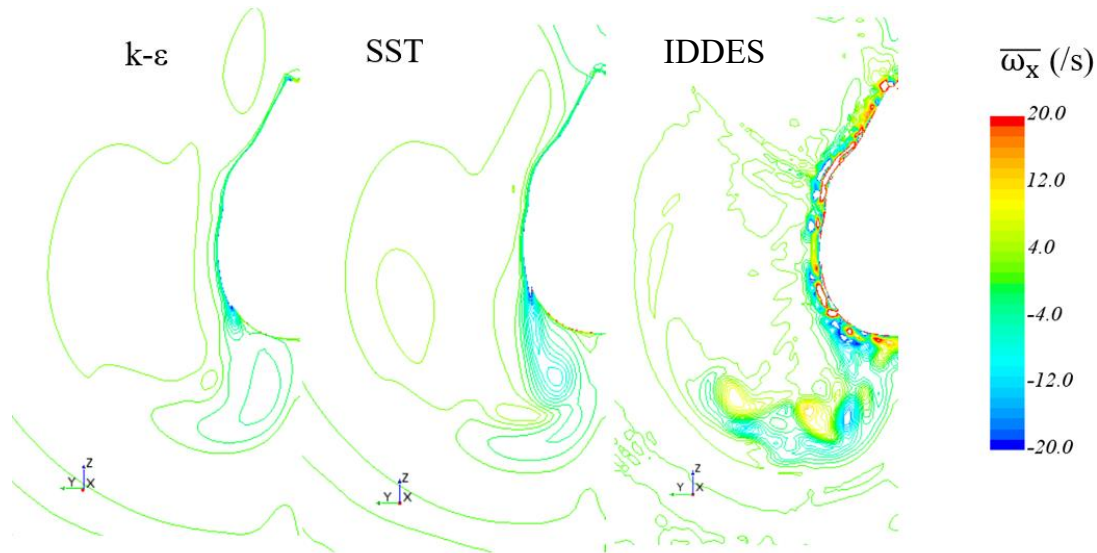


Figure 8 Iso-lines of streamwise vorticity at $x/L=0.03$ (upstream of the propeller plane) for the three turbulence modelling strategies

Substantial vorticity disparities upstream of the propeller suggest that significant differences could also be present in the propeller region. In Figure 9, vorticity magnitude contours are shown in the propeller plane. Although all models calculated a hook-shaped bilge vortex, it is visible that the $k-\epsilon$ generated the weakest bilge vortex, followed by the SST and the IDDES. The vorticity fields analysis has revealed that at full scale, the IDDES calculates a stronger bilge vortex, and confirms that the intensity of the bilge vortex is dependent upon the chosen turbulence model strategy. This conclusion contradicts the 2000 Gothenburg Workshop (Larsson et al., 2003), but is in line with the Starke et al. (2006) investigations.

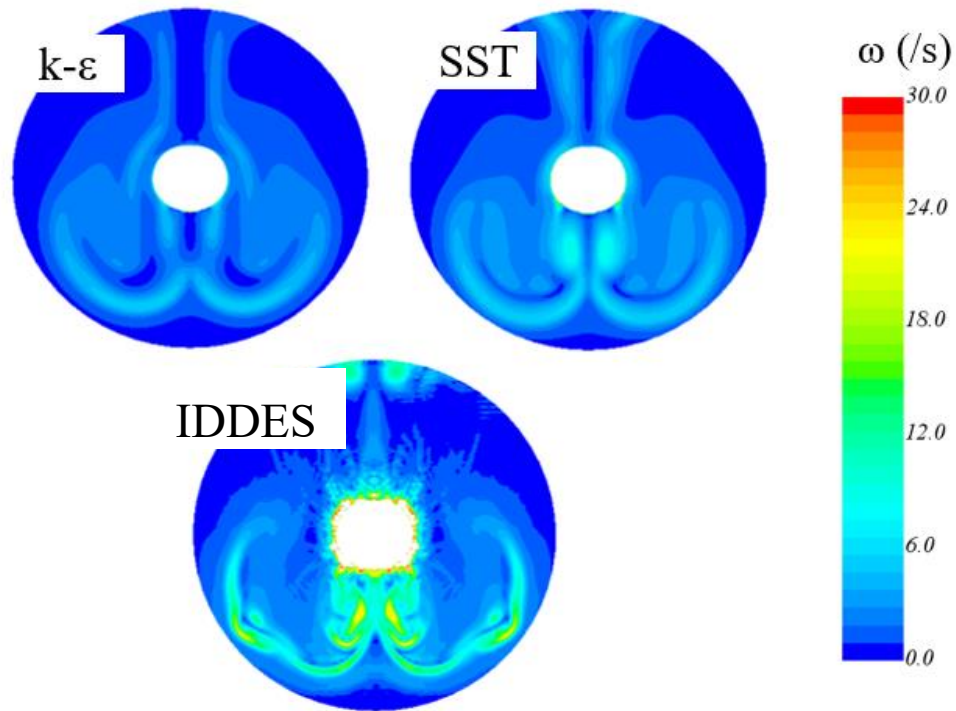


Figure 9 Vorticity magnitude at the propeller disk for the three turbulence modelling strategies

7.3. Nominal Wake Field

The intensity of the bilge vortex disparity, as seen in Figure 9, was expected to be reflected in the velocity contours at the nominal wake region. Looking at the vorticity contours, it was anticipated that the distortion of the velocity field due to the bilge vortex would also result in a hook-shaped velocity field. Figure 10 shows the iso-lines (contours) of the dimensionless axial velocity ($\frac{\bar{u}_x}{U_\infty}$). Both RANS set-ups demonstrated a fair agreement. Differences were observed in the region closer to the propeller centre, where stronger velocity retardation and a higher degree of three dimensionality of the wake field was seen for the SST model. On the other hand, the hybrid IDDES model showed close to zero velocity fluid on the region under the shaft. The explanation for the velocity field difference has its origin in the vorticity fields shown in Figure 8 and Figure 9. The k- ϵ bilge vortex was the weakest and, therefore, the calculated axial velocity at the propeller disk reflected a less disturbed fluid. By contrast, for the IDDES set-up a stronger vortex produced a higher disturbance of the flow and therefore induced much lower velocity fields at the propeller region.

Overall, this investigation demonstrated that at full scale insufficient resolution of vortex structures shed from the hull results in an underestimation of the wake non-uniformity. Also, the underestimation of the bilge vortex had a large effect on the boundary layer velocity field around the ship and the calculated torque in full scale.

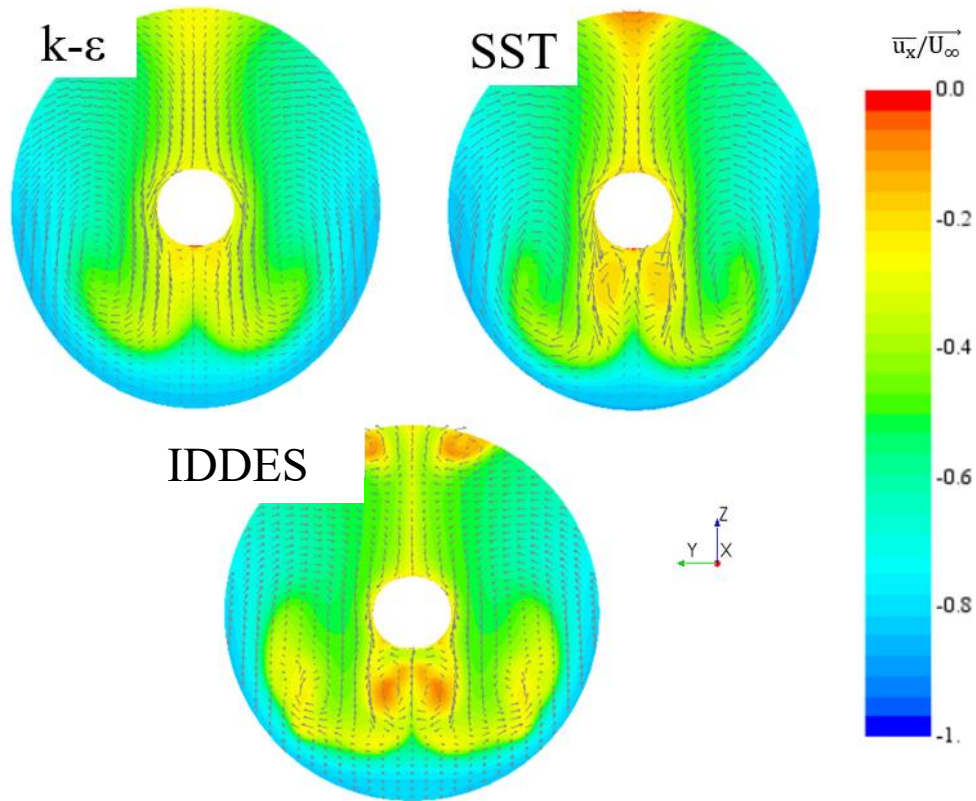


Figure 10 Nominal wake fields for the three turbulence modelling strategies

8. Conclusions

The present research has investigated which numerical approach is able to provide an accurate and detailed picture of the boundary layer and wake of a full-scale ship. Two RANS turbulence modelling approaches, suitable for the simulation of ship flows have been assessed: the $k-\epsilon$, $k-\omega$ SST together with an IDDES approach. During this study, very fine meshes suitable for sophisticated turbulence modelling strategies were implemented.

Whilst RANS is widely used for the prediction of the hydrodynamic performance of energy saving devices that work within the boundary layer and wake of a ship (J.P Chen *et al.*, 2014; Jung-Eun Choi *et al.*, 2015; Mizzi *et al.*, 2017), this work showed that RANS numerical simulations in full scale resulted in a less accurate prediction of the velocity fields within the ship boundary layer and wake. It is therefore possible that using RANS as a turbulent modelling strategy could be linked to known issues and discrepancies between sea trials and numerical simulations of energy saving devices performance (ITTC, 2014a).

This investigation has revealed that the IDDES numerical model replicated the sea trial measurements with the highest degree of accuracy. This finding provides confidence that the hydrodynamics of the boundary layer and wake around the ship were accurately resolved for the IDDES case. Also, this finding proved that the accurate resolution of the bilge vortex is crucial when calculating the propeller torque. Therefore, to overcome numerical errors, the IDDES-based numerical approach presented in this work is recommended for the investigation of the wake and boundary layer of full scale ships with particular focus on the design of propellers, rudders or energy saving devices.

As future work, the authors are conducting boundary layer studies using the IDDES approach in order to further assess its enhanced capabilities when used for calculating wakes. It would also be beneficial to study the suitability of other Zonal Detached Eddy Simulations approaches, such as ZDES, for the calculation of nominal wakes, since it could offer computational savings when compared to the IDDES approach.

References

- Aloisio G., F. F. (2006) ‘PIV analysis around the Bilge Keel of a Ship Model in Free Roll Decay’, in *XIV Convegno Nazionale A.I.V.E.L.A.*, pp. 6–7. Available at: <http://www.insean.it>.
- Andersson, J. *et al.* (2015) ‘CFD Simulations of the Japan Bulk Carrier Test Case’, in

Proceedings of the 18th Numerical Towing Tank Symposium.

Arolla, S. K. and Durbin, P. A. (2013) ‘Modeling rotation and curvature effects within scalar eddy viscosity model framework’, *International Journal of Heat and Fluid Flow*, 39, pp. 78–89. doi: 10.1016/j.ijheatfluidflow.2012.11.006.

Chen, J.P., Su, J., Yang, L. (2016) ‘Investigation On Propulsion And Flow Field Of Ships With Energy Saving Devices Using Cfd Predictions And Model Tests’, in *The 12th International Conference on Hydrodynamics*. Available at: <https://api.semanticscholar.org/CorpusID:128008005>.

Doligalski, T. (2002) ‘Vortex Interactions with Walls’, *Annual Review of Fluid Mechanics*, 26(1), pp. 573–616. doi: 10.1146/annurev.fluid.26.1.573.

Dousset, V. and Pothérat, A. (2010) ‘Formation mechanism of hairpin vortices in the wake of a truncated square cylinder in a duct’, *Journal of Fluid Mechanics*, 653, pp. 519–536. doi: 10.1017/S002211201000073X.

IMO (2020) *Low Carbon Shipping and Air Pollution Control*. Available at: <http://www.imo.org/en/MediaCentre/HotTopics/GHG/Pages/default.aspx>.

ISO (2015) *ISO 15016:2015 Standard, Ships and marine technology — Guidelines for the assessment of speed and power performance by analysis of speed trial data*. Available at: <https://www.iso.org/standard/61902.html>.

ITTC (2014a) ‘27th Propulsion Committee Proceedings’, in *27th ITTC 2014*.

ITTC (2014b) ‘ITTC – Recommended Procedures and Guidelines Preparation and Conduct of Speed / Power Trials 7.5-04-01-01.1’, in *27th ITTC 2014*.

ITTC (2014c) ‘Practical guidelines for RANS calculation of nominal wakes. 7.5-03-03-02’, in *27th ITTC 2014*, p. 9.

ITTC (2014d) ‘Quality System Manual Recommended Procedures and Guidelines Practical Guidelines for Ship CFD Applications 7.5-03-02-03’, in *27th ITTC 2014*.

ITTC (2017) ‘Uncertainty Analysis in CFD Verification and Validation Methodology and Procedures 7.5-03 -01-01’, in *28th ITTC 2017*.

Jasak, H. *et al.* (2019) ‘CFD validation and grid sensitivity studies of full scale ship self propulsion’, *International Journal of Naval Architecture and Ocean Engineering*, 11(1), pp. 33–43.

Jeong, J. and Hussain, F. (1995) ‘On the identification of a vortex’, *Journal of Fluid Mechanics*, 285, pp. 69–94. doi: 10.1017/S0022112095000462.

Kim, J. H. *et al.* (2015) ‘Development of Energy-Saving devices for a full Slow-Speed ship through improving propulsion performance’, *International Journal of Naval Architecture and Ocean Engineering*, 7(2), pp. 390–398. doi: 10.1515/ijnaoe-2015-0027.

Kolmogorov, A. N. (1941) ‘The Local Structure of Turbulence in Incompressible Viscous Fluid for Very Large Reynolds Numbers’, *Proceedings of the Royal Society A: Mathematical, Physical and Engineering Sciences*, 434(1890), pp. 9–13. doi: 10.1098/rspa.1991.0075.

Larsson, Lars; Stern, Frederick; Bertram, V. (2003) ‘Benchmarking of Computational Fluid Dynamics for Ship Flows: The Gothenburg 2000 Workshop’, *Journal of Ship Research*, 47(1), pp. 63–81.

Larsson, L., Stern, F. and Visonneau, M. (2013) *Numerical ship hydrodynamics: an assessment of the Gothenburg 2010 workshop*. Springer.

Lim, S. S. *et al.* (2014) ‘Parametric study of propeller boss cap fins for container ships’, *International Journal of Naval Architecture and Ocean Engineering*, 6(2), pp. 187–205. doi: 10.2478/IJNAOE-2013-0172.

Lloyds Register (2016) ‘Workshop on Ship Scale Hydrodynamic Computer Simulation Proceedings’, in.

Menter, F. R. (1993) ‘Zonal Two Equation $k-\omega$ Turbulence Models for Flows’, in *24th AIAA Fluid Dynamics Conference*, pp. 93 – 2906.

Mizzi, K. *et al.* (2017) ‘Design optimisation of Propeller Boss Cap Fins for enhanced propeller performance’, *Applied Ocean Research*, 62, pp. 210–222. doi: 10.1016/j.apor.2016.12.006.

Nishino, T., Roberts, G. T. and Zhang, X. (2008) ‘Unsteady RANS and detached-eddy simulations of flow around a circular cylinder in ground effect’, *Journal of Fluids and Structures*, 24(1), pp. 18–33. doi: 10.1016/j.jfluidstructs.2007.06.002.

Pena, B., Muk-Pavic, E. and Ponkratov, D. (2019) ‘Achieving a high accuracy numerical simulations of the flow around a full scale ship’, in *Proceedings of the International Conference on Offshore Mechanics and Arctic Engineering - OMAE*. doi: 10.1115/OMAE2019-95769.

Ponkratov, D. and Zegos, C. (2015) ‘Validation of Ship Scale CFD Self-Propulsion Simulation by the Direct Comparison with Sea Trials Results’, in *Fourth International Symposium on Marine Propulsors*. Available at: <http://www.marinepropulsors.com/proceedings/2015/TB1-1.pdf>.

Pope, S. B. (2000) *Turbulent Flows*. Cambridge University Press 1st Edition. doi:

10.1017/CBO9780511840531.

Sakamoto, H. and Haniu, H. (1990) 'A study on vortex shedding from spheres in a uniform flow', *Journal of Fluids Engineering, Transactions of the ASME*, 112(4), pp. 386–392. doi: 10.1115/1.2909415.

Shur, M. L. *et al.* (2008) 'A hybrid RANS-LES approach with delayed-DES and wall-modelled LES capabilities', *International Journal of Heat and Fluid Flow*, 29(6), pp. 1638–1649. doi: 10.1016/j.ijheatfluidflow.2008.07.001.

Spalart, P. R. *et al.* (2006) 'A new version of detached-eddy simulation, resistant to ambiguous grid densities', *Theoretical and Computational Fluid Dynamics*, 20(3), pp. 181–195. doi: 10.1007/s00162-006-0015-0.

Starke, B., Windt, J. and Raven, H. C. (2006) 'Validation of viscous flow and wake field predictions for ships at full scale', in *Symposium of Naval Hydrodynamics*, pp. 17–22.

Thornber, B., Starr, M. and Drikakis, D. (2010) 'Implicit large eddy simulation of ship airwakes', *Aeronautical Journal*, 114(1162), pp. 715–736. doi: 10.1017/S0001924000004218.

Xing, T., Carrica, P. and Stern, F. (2010) 'Large-Scale Rans and Ddes Computations of Kvlcc2 At Drift Angle 0 Degree', (3), pp. 2–7.